Desalination and Water Treatment
www.deswater.com

doi: 10.5004/dwt.2019.23997

155 (2019) 94–112
July

Nutraceutical industrial chillies stalk waste as a new adsorbent for the removal of Acid Violet 49 from water and textile industrial effluent: adsorption isotherms and kinetic models

Syida Aameera Yakuth[a], Syed Noeman Taqui[b], Usman Taqui Syed[c], Akheel Ahmed Syed[a,*]

[a]*Department of Studies in Chemistry, University of Mysore, Manasa Gangothri, Mysuru-570006, India, Tel. +91-7338004134; emails: akheelahmed54@gmail.com (A.A. Syed), yakuth2apr@gmail.com (S.A. Yakuth)*
[b]*Department of Chemistry, University of Malaya, Kuala Lumpur-50603, Malaysia, email: noemansyed89@gmail.com*
[c]*LAQV-REQUIMTE, Department of Chemistry, Faculty of Science and Technology, Universidade NOVA de Lisboa, 2829-516 Caparica, Portugal, email: s.taqui@campus.fct.unl.pt*

Received 23 January 2018; Accepted 19 February 2019

ABSTRACT

First-ever study on the adsorption of Acid Violet 49 (AV49) dye, onto nutraceutical industrial chillies stalk waste (NICSW) is reported. A two-level fractional factorial experiment design and analysis of variance (ANOVA) were adopted to study how initial concentration of the dye, adsorbent dosage, duration of adsorption process, speed of agitation, pH of the reaction mixture and temperature affect the adsorption process. The adsorption capacity of NICSW at equilibrium was analyzed using Langmuir, Freundlich, Jovanovic, Temkin, Dubinin–Radushkevich and Harkins–Jura isotherms. The pseudo-first-order and pseudo-second-order models were considered for kinetic studies. Maximum adsorption capacity of 45.40 mg/g was obtained by Langmuir isotherm as against the experimental value of 29.00 mg/g, with correlation coefficient of 0.979 at near neutral pH. NICSW was characterized by Fourier transform infrared spectroscopy, Brunauer–Emmett–Teller, scanning electron microscope and energy dispersive X-ray spectroscopy. Elemental (C, H, N, S) analyses of the adsorbent were conducted. Along with thermodynamic parameter evaluation such as Gibb's free energy, enthalpy and entropy and results of the surface characterization showed that the dye adsorption onto the biosorbent has taken place such as a physical process. These results proved that NICSW is a fast and effective adsorbent to remove AV49 from water and textile industrial effluent.

Keywords: Nutraceutical industrial waste; Chillies stalk waste; Biosorption; Acid Violet 49 dye; Adsorption isotherms; Kinetics; Textile industrial effluent

1. Introduction

Chilli (*Capsicum annuum* L.) or red pepper is an important condiment or vegetable cultivated in several parts of the world. There are more than 400 chilli varieties existing all over the world and it is an important cash crop. Originally it belonged to tropical America and West Indies from where it was introduced to India in 17th century by the Portuguese [1]. Since then, it has become an essential part of Indian cuisine and it is valued for its characteristic pungency, color and aroma.

The total production of chillies around the world is almost 7 million ton, being cultivated in 1.5 million ha [2]. India is the world's largest producer of chillies with annual production of about 1.7 million tonnes and grown as an annual crop in 1.40 lakh ha [2]. Chillies are exported as dried produce, chillies powder, pickled chillies and chillies oleoresin. Chillies oleoresins are gaining importance as it is convenient to standardize the quality and strength of flavour.

Chilli fruit parts are shown in Fig. 1(a). The stalk and calyx (Fig. 1(b)) comprise 5%–10% of the total weight of the

* Corresponding author.

fruit and they are separated prior to processing for extraction of oleoresin. The stalks have neither fertilizer nor feed value. Due to traces of pungency incineration and burning is not feasible. The amount of stalk along with calyx generated as waste in industries amounts to thousands of tonnes which need to be disposed properly on priority. The chillies stalk waste powder is shown in Fig. 1(c).

Textile industry is one amongst the top 10 polluting industries [3]. About 50,000 tons of synthetic dyes are entering the water systems due to improper processing and dying methods adopted by textile industries [4]. Synthetic dyes are mostly carcinogenic, mutagenic and/or teratogenic and can cause severe damage to human beings [5]. Thus, removal of dyes from textile effluent before it is discharged into receiving water bodies assumes paramount importance [6]. Furthermore, recalcitrance nature and undesirable color of the dyes will restrict sunlight penetration and obstruct photochemical and biological metabolism thereby causing destruction of aquatic life [7].

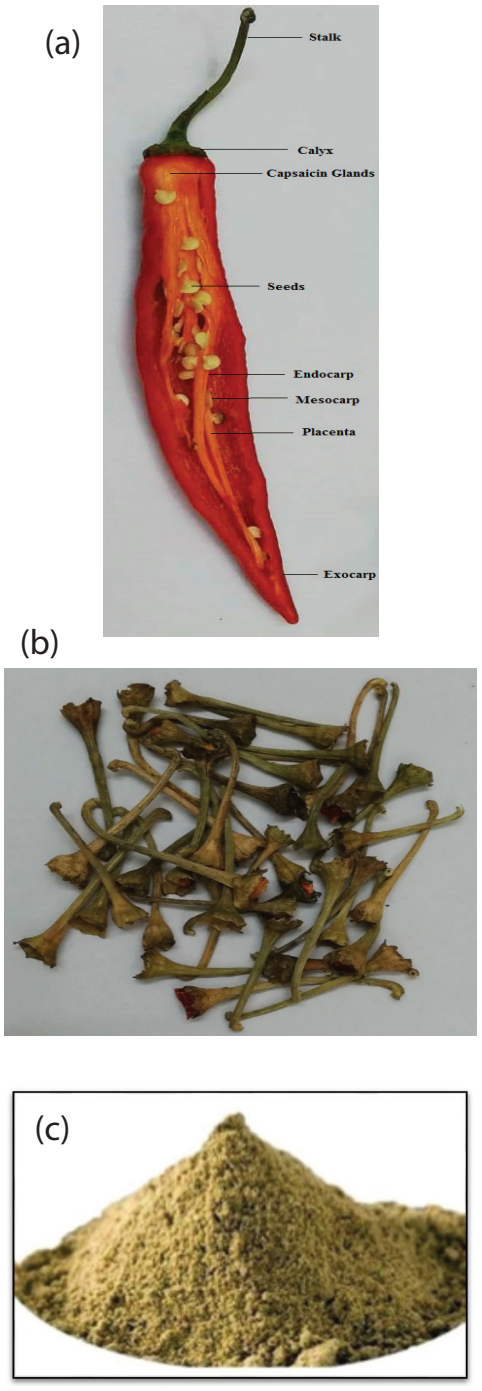

Fig. 1. (a) Parts of chillies fruit, (b) chillies stalk and (c) nutraceutical industrial chillies stalk waste powder.

The techniques, methods and procedures reported in the literature for remediation of synthetic dyes can be broadly classified into three major groups; these are biological, chemical and physical methods. Use of microorganisms [8–13], nano materials [14–18], blends and polymers [19–21] and degradation techniques such as sonochemical [22], electrochemical [23] and oxidative degradation [24] are reported in the literature. These methods have such problems as high quantity of cost, operational difficulties including creation of toxic intermediates, lower quantity of removal and increased specificity for some dyes and such others [25].

Adsorption, technique being easy to operate and less cost involvement, regeneration, recovery and recycling possibilities have shown it a prominent technique to separate dyes from aqueous systems [26–28]. Adsorption by activated carbon has proved the best and widely used technique for dye removal [29–31], but its high cost and regeneration problems, search for alternatives with low-cost continues. As the wastewater produced by the textile industries is of large quantity, research at present for novel low-cost and ready-to-use adsorbent(s) is in progress.

An ideal biosorbent for remediation of dyes from industrial effluents should have the following characteristics: It should be available in abundance; it should have no or minimal use(s) which may result in increase in price due to demand; it should be ready-to-use without any pre-chemical treatment and it should have pore structure to have better adsorption. To match the volume of effluents generated in textile industries, and the parameters listed above, the nutraceutical industrial waste (NIW) and nutraceutical industrial spent obtained in myriad tons will cater to the demand.

The expansion of nutraceutical sector is fast and according to the global nutraceutical product market is expanding at a compound annual growth rate (CAGR) of 7.3% from 2015 to 2021 which was valued at US$ 182.6 bn in 2015, is going to reach US$ 278.95 bn by the end of 2021 as per the transparency market research https://www.transparencymarketresearch.com/global-nutraceuticals-product-market.html (Accessed on 18 April 2019). The nutraceutical industry is facing a great problem of disposing waste which accounts for 50%–95% of the total raw materials covering different types of herbs, shrubs, seeds and/or roots after being processed to get the active ingredient(s).

Nutraceutical industrial fennel seed spent has been tried for the remediation of Congo red dye [32], ethidium bromide [33] and nutraceutical industrial saw palmetto spent for the remediation of methylene blue [34]. The vast amount of published reports on adsorption of dyes using low-cost biological materials did not indicate any methods for the reuse of resulting "sludge". A feasible solution to dispose off the dye-adsorbed "sludge" is to incorporate the same in

petroleum-based non-biodegradable thermoplastics thereby generate green composites lowering the use of plastics and reducing carbon footprint [32,35]. By combining lignocellulosic materials with plastics, it is possible to get many environmental friendly benefits including making of light weight final product, lowering the manufacturing machinery erosion, cost reduction, biodegradability and prevention/minimization of burnt residue production or toxic by-products. Our research school has reported about this aspect [36–43].

Acid Violet 49 (AV49) dye (Fig. 2) belongs to the class of triarylmethane dyes, extensively used for dyeing wool, silk and polyamide fiber for its better color performance. Survey of literature revealed that no work on remediation of AV49 dye as well as use of chillies stalk waste as adsorbent has been so far reported. This paper attempts to use nutraceutical industrial chillies stalk waste as an adsorbent for the bioremediation of AV49 dye which is a toxic dye used in the textile industries and finally discharged as a pollutant to the environment.

2. Materials and methods

2.1. Materials

Commercial sample of the dye, Acid Violet 49 dye (C.I. = 42,640; chemical formula = $C_{39}H_{40}N_3NaO_6S_2$; molecular weight = 733.87; absorbance maximum [λ_{max}] = 549 nm) was procured from local manufacturers, India. AV49 dye is a bright blue purple powder. It readily dissolves in cold and hot water and soluble in ethanol. In these three solvents, it retains its purple color. At higher concentrations of sulfuric acid, it turns to orange color which upon dilution turns to mustard color. The AV49 dye stock solution of dye was made by dissolving exact amount of the dye in distilled water. Further solutions of needed concentrations were prepared by diluting the stock solution using double distilled water. The chemicals used for all these studies were of analytical grade.

2.2. Determination of molar extinction coefficient (ε) of AV49

Nine different concentrations (0.20×10^{-4}; 0.40×10^{-4}; 0.60×10^{-4}; 0.80×10^{-4}; 1.00×10^{-4}; 1.20×10^{-4}; 1.40×10^{-4}; 1.60×10^{-4} and 1.80×10^{-4}) of AV49 dye were prepared in distilled water and absorbance was measured at 549 nm along with distilled water as reference using UV–Vis spectrophotometer (Lambda 25, PerkinElmer, USA). A graph of absorbance vs. concentration was plotted (Fig. 3). ε was measured from the slope of the linear portion of the curve or by using mathematical formula ε = *A*/*Cl* where, *A* is specific absorption coefficient for concentration *C* (mol/L) for a path length of 1-cm. Specific absorption coefficient or absorbency index is the absorbance per unit path length and unit concentration. In case of the latter the ε_{AV49} dye was calculated as the mean of nine values:

$$\varepsilon_{AV49} = \varepsilon_1 + \varepsilon_2 + \varepsilon_3 + \varepsilon_4 + \varepsilon_5 + \varepsilon_6 + \varepsilon_7 + \varepsilon_8 + \varepsilon_9/9$$

$$\varepsilon_{AV49} = 15{,}844 + 16{,}238 + 16{,}443 + 16{,}758 + 17{,}120 + 17{,}487 + 17{,}867 + 18{,}275 + 18{,}250/9 = 17{,}142$$

The low value of ε_{AV49} dye is attributed to the low content of azo dye in a commercial sample.

2.3. Adsorbent preparation

Nutraceutical industrial chillies stalk waste (NICSW) was obtained from a local industry to get sample as close to real world application as possible. The NICSW was dried in sunlight and ground by a ball mill to fine powder. The NICSW powder was sieved to pass through ASTM 80 mesh and the obtained particle sizes were of ≤177 μm.

2.4. Characterization of NICSW

Characterization of NICSW elemental (C, H, N, S) analyses was conducted using Euro EA elemental analyzer (HEKA tech, GmbH, Germany), which gave 68.56%C, 29.67%H, 1.71%N and 0.056%S. Fourier transform infrared spectra were recorded in the 4,000–600 cm^{-1} region by a PerkinElmer Spectrum two, USA, Fourier transform infrared (FTIR) spectrometer.

The surface charge of NICSW was determined by preparing stock solution of 0.1 M KCl. 50 mL each of 0.1 M KCl were transferred to seven 250-mL Erlenmeyer flasks and pH was adjusted initially to 2.0 and 12.0 by using HCl and NaOH. NICSW (0.05 g) was added to each flask. After allowing for 24 h, the final pH was measured by pH meter (Systronics-802, India). Graph of pH_{final} vs. $pH_{initial}$ was plotted. The point of zero charge for NICSW was found to be pH 7.20.

Measurement of pore and surface characteristics was done by N_2 adsorption at 77 K using a BELSORP, Japan, surface area analyzer (Fig. 4). Adsorption isotherms were carried out at saturated vapor pressure of 94.741 kPa.

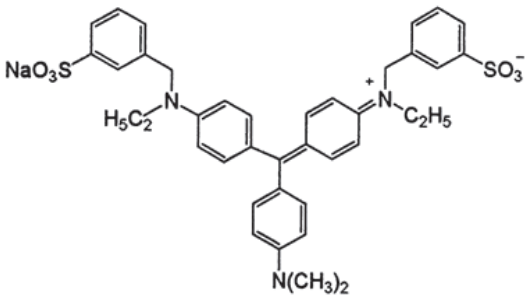

Fig. 2. Structure of Acid Violet 49 dye.

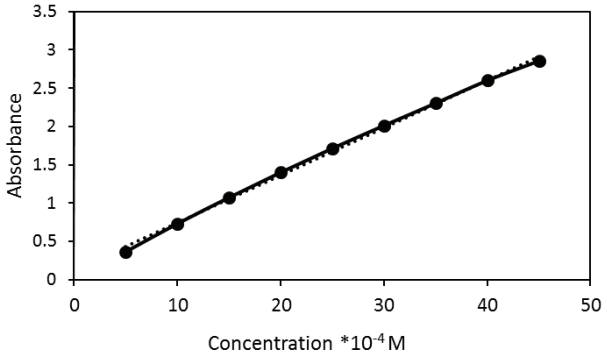

Fig. 3. Determination of molar extinction coefficient of AV49 dye by spectrophotometric method.

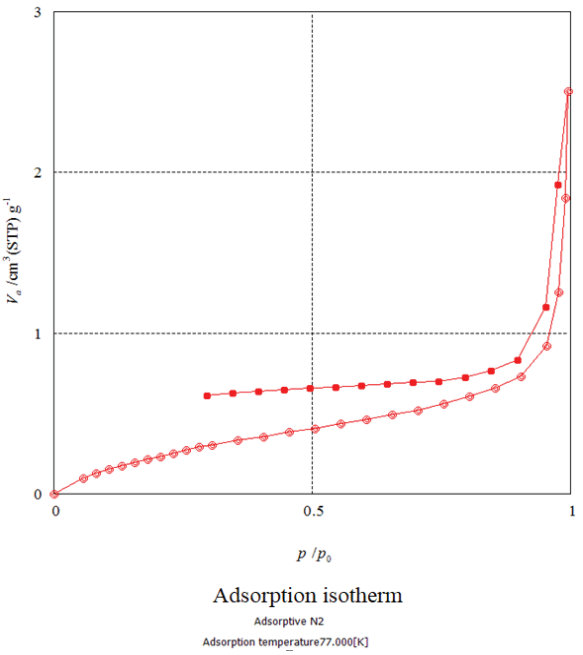

Fig. 4. Adsorption isotherm of NICSW.

The Brunauer–Emmett–Teller (BET) monolayer volume, V_m, energy constant, C, mean pore diameter, d_p, specific surface area, a_{sBET} and total pore volume, V_p was estimated from a relative pressure of 0.990. The BET values were compared with values derived from Langmuir plot and MP plot. The distribution of pore size was constructed for which desorption data points were analyzed using Barrett–Joyner–Halenda (BJH) and Dollimore Heal (DH) methods.

The adsorbent surface morphology was visualized by scanning electronic microscope (SEM; Hitachi S-3400N, Japan). Scanning electronic microscope energy dispersive X-ray spectrometer (SEM-EDS) was used in order to determine NICSW chemical composition (Figs. 5(a)–(c)).

2.5. Batch adsorption experiments

All batch adsorption experiments were done in 250-mL flasks with 50 mL working aqueous solution of AV49 dye and 50 mg of the adsorbent (NICSW). The flasks were agitated at a constant speed of 175 rpm for 3 h in a temperature controlled shaker. Various parameters effects at varying levels such as pH (2, 4, 6, 7, 8, 10 and 12), initial AV49 dye concentration (25, 50, 75, 100, 125, 150, 175 and 200 mg/L), time on adsorption process (15, 30, 45, 60, 90, 120, 150, 180 min), adsorbent dosage (0.025, 0.050, 0.075, 0.100, 0.150, 0.200, 0.300 g/50 mL), speed of agitation (75, 100, 125, 150, 175, 200 rpm) and temperature (303, 313 and 323 K) were evaluated. After the predetermined contact time, samples were centrifuged for 5 min at 3,000 rpm till a clear supernatant liquid was obtained. If the solution is not clear, additional 5 min centrifugation was performed. The concentration of AV49 dye in the supernatant solution was measured at 549 nm using UV–Vis spectrophotometer (PerkinElmer-Lambda 25, USA). Controls were maintained using adsorbent in distilled water and adsorbent-free AV49 dye. The adsorbed amount of

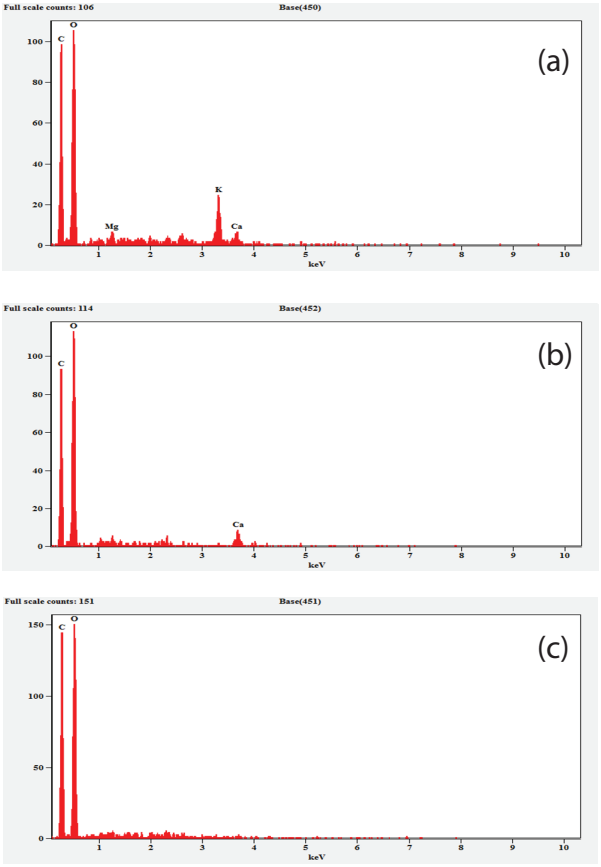

Fig. 5. Energy dispersive X-ray spectrometric analysis of (a) NICSW before adsorption, (b) AV49–NICSW and (c) spiked and dried AV49–NICSW with TIE.

AV49 dye at equilibrium q_e (mg/g), at a given time q_t (mg/g) and percentage removal (R%) of the dye from aqueous solutions was determined using the equations:

$$q_e = (C_0 - C_e)V/W \quad (1)$$

$$q_t = (C_0 - C_t)V/W \quad (2)$$

$$R\% = (C_0 - C_t/C_0) \times 100 \quad (3)$$

where C_0, C_e and C_t are the concentrations (mg/L) of AV49 dye at initial, at equilibrium and at time t, respectively. V is the volume (L) of the solution and W is the weight (g) of the adsorbent used. All the adsorption experiments were performed in triplicate and the mean values were used in data analysis. Control experiments were performed with the addition of NICSW. The results confirmed that the adsorption of the dye on the walls of conical flasks was negligible.

2.6. Statistical optimization of process parameters

The factors affecting the final adsorption process studied included adsorption time (A), process temperature (B), initial dye concentration (C), agitation speed (D), adsorbent dosage (E) and pH (F). The statistical FFED chosen covered six factors at two levels (Table 1). ANOVA was conducted with the

Table 1
Fractional factorial experiment designs – low and high level factors

Factor	Name	Units	Minimum	Maximum
A	Time of contact between adsorbent and adsorbate	Minute	15	180
B	Temperature of the process	°C	27	50
C	Initial dye concentration	mg/L	25	200
D	Agitation speed	rpm	75	200
E	Absorbent dosage	g/L	0.500	6.000
F	pH		2	12

Table 2
Surface characterization of NICSW using different methods

BET analysis		Langmuir plot		MP plot		BJH plot		DH plot	
V_m	0.2689	V_m	0.4730	V_p	1.2559E-04	r_p	1.29	r_p	1.29
a_{aBET}	1.1703E+00	a_{aLang}	2.0589	a_1	0.4459	a_p	1.2508	a_p	1.3557
C	8.7164	B	5.2907E-02	a_2	0.7178	V_p	3.2061E-03	V_p	3.2846E-03
V_p	3.0012E-03								

results which were followed by preparing a general quadratic regression equation. This equation was used for optimization as per FFED. The effects of individual parameters and their interactions on adsorption capacity were indicated by surface and contour plots.

3. Results and discussion

3.1. Characterization of the adsorbent

3.1.1. Surface characterization

The surface characterization of NICSW and AV49–NICSW (Fig. 6) was conducted through SEM–EDS (Fig. 5). As can be seen from Fig. 5, the adsorbent is not only efficient in adsorbing the dye but also has potential to remove various constituents including metal ions from the industrial effluent.

BET method is probably the most widely used method for surface area characterization of agriculture biomass. It involves the procedure of adsorption of nitrogen at a saturated vapor pressure of 94.741 kPa and temperature of 77 K. BET method is sensitive and reliable as it is least influenced by surface chemistry. However, this method is different from BJH and DH methods as the latter determine pore size distribution of mesoporous solids based on Kelvin equation. To enhance the reliability of the results of the above methods, the authors have also carried out Langmuir plot and MP plot. The results are tabulated and presented in Table 2. BET plot, Langmuir plot, MP plot, BJH plot and DH plot of NICSW are presented as Figs. S1–S5.

3.1.2. FTIR analysis

Infrared spectroscopy, an analytical technique also known as vibrational spectroscopy is extensively used to elucidate the functional groups of inorganic and organic compounds. This technique is used to elucidate the information about active surfaces of many lignocellulosic materials.

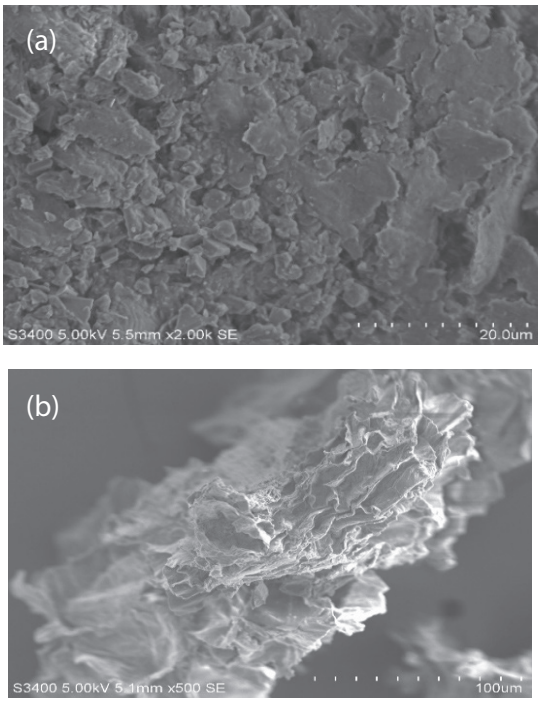

Fig. 6. SEM image of (a) NICSW and (b) AV49–NICSW.

In the present case, the technique has been used to get the information about the functional groups and the possibilities of binding of dye molecule on NIW. This has been done by recording the spectra of NICSW, AV49 dye and dye-adsorbed NICSW. The spectra are displayed in Figs. 7(a)–(c).

The broadband between 3,100 and 3,500 cm^{-1} in the IR spectrum of NICSW is attributed to the hydroxyl groups of cellulose and adsorbed water molecule. A strong band observed at 3,339 cm^{-1} testifies to –OH stretching and possibilities of the formation of various types of hydrogen bonds which helps in stabilizing certain conformation

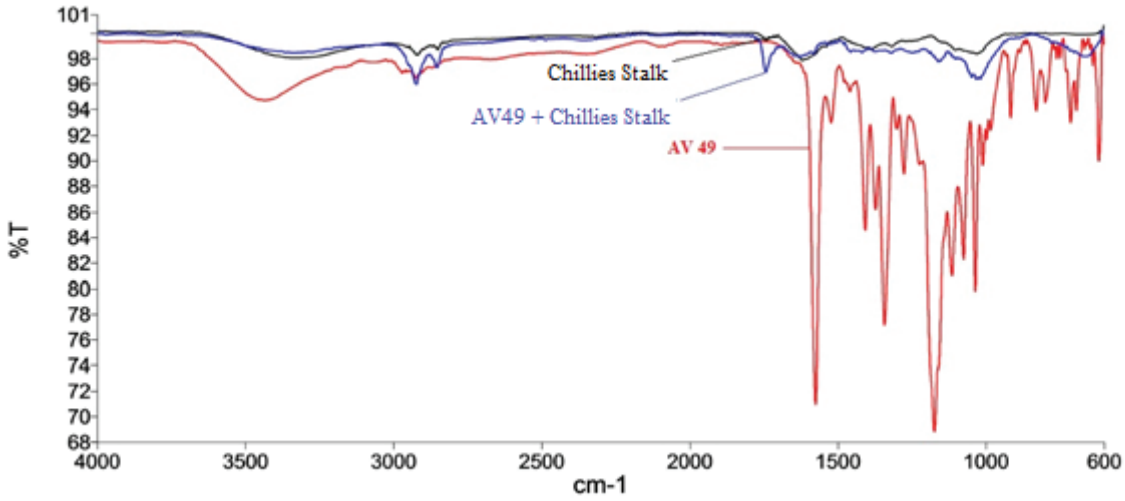

Fig. 7. FTIR spectra of (a) AV49 dye; (b) NICSW and (c) AV49 dye-adsorbed NICSW.

macromolecules present in NICSW. The bands at 2,924 and 2,851 cm^{-1} are ascribed to aliphatic C–H of carboxylic acid. The bands at 1,621 and 1,775 cm^{-1} are ascribed to C=O antisymmetric stretching vibration of lignin. A doublet at 1,390 cm^{-1} and a peak at 1,310 cm^{-1} may be ascribed to C–O–C/C–O (ester, ether and phenolic groups). A weak band at 2,923 cm^{-1} is due to the C–H stretching and band at 1,607 cm^{-1} is due to C–O stretching. Further, the bands at 1,365; 1,317; 1,298; 1,258 and 1,026 cm^{-1} are attributed to the C–O–C stretching.

The IR spectrum of AV49 dye adsorbed on NICSW exhibits broad bands between 3,300 and 34,50 cm^{-1} and these are attributed to N–H stretching of $–N(CH_3)_2$ group in AV49 dye and the disappearance of the band between 3,100 and 3,500 cm^{-1} is due to the formation of hydrogen bonds with hydroxyl groups of NICSW and $–N(CH_3)_2$. In addition, the disappearance of a strong peak at 1,576 cm^{-1} for C=N stretching and weak peaks at 1,519 and 1,343 cm^{-1} for C=C stretching in aromatic ring of AV49 dye also confirm the strong adsorption of AV49 dye on NICSW. The shift in peaks of AV49 dye-adsorbed NICSW and vis-à-vis NICSW AV49 dye manifest that interactions have taken place between the dye and the adsorbent.

3.2. Batch adsorption studies

3.2.1. Effect of initial dye concentration

The rate of adsorption is an important parameter and it is dependent on the initial dye concentration. The studies on this parameter were carried out using a fixed adsorbent dosage (50 mg) in 50 mL of the dye solution at pH 7.0. The q_e value increased from 7 to 30 mg/g as the AV49 dye concentration in the test solution was increased from 25 to 200 mg/L. Higher adsorption capacity by NICSW was evident with increase in dye concentration from 25 to 100 mg/L and thereafter the increase was marginal up to 200 mg/L (Fig. 8(a)). This observation commensurate with the chemistry of the adsorbent as the rate of adsorption is faster initially due to the adsorption of the dye onto the active sites of the adsorbent. Further increase in dye concentration though enhances the interaction between the dye and adsorbent apart from providing necessary driving force to overcome the resistance to mass transfer of dye, the already partial filled active sites retard the rate of adsorption and hence dye uptake increase was marginal with increase in dye concentration from 100 to 200 mg/L.

3.2.2. Effect of adsorbent dosage

Adsorbent dose affects the adsorption process and determining the adsorption capacity of adsorbent at the operating conditions. The adsorption percentage and amount adsorbed increased with the increase in adsorbent dose from 0.025 to 0.500 g/50 mL of dye solution. From Fig. 8(b), it is clear that increase in dye adsorption capacity was evident when the adsorbent dose increased from 0.025 to 0.050 g/50 mL dye solution. This is attributed to increase in the surface area of the adsorbent. Thereafter, the amount of adsorption decreased which is attributed to two factors. First, overlapping or aggregation of adsorption sites resulting in a decrease in the total adsorbent surface area available to AV49 dye and second, increase in diffusion path length.

3.2.3. Effect of time on adsorption process

The percentage AV49 dye removal as a function of time was studied in the range of 15–180 min with initial concentration of 100 mg/L of dye and adsorbent dosage of 0.050 g/50 mL of 100 mg/L dye solution (Fig. 8(c)). The q_e value reached 27.00 mg/g in 120 min. Further increase in contact time up to 180 min marginally increased the q_e value (30.00 mg/g). To optimize the condition and save energy cost, 120 min of contact time was chosen for all studies.

3.2.4. Effect of agitation speed

Agitation is an important factor for the adsorption of the dye molecule onto a cellulosic material as it influences the distribution of dye molecule in bulk solution and formation of the boundary film. Fig. 8(d) shows the adsorption capacity of NICSW. The agitation speed was increased from 75

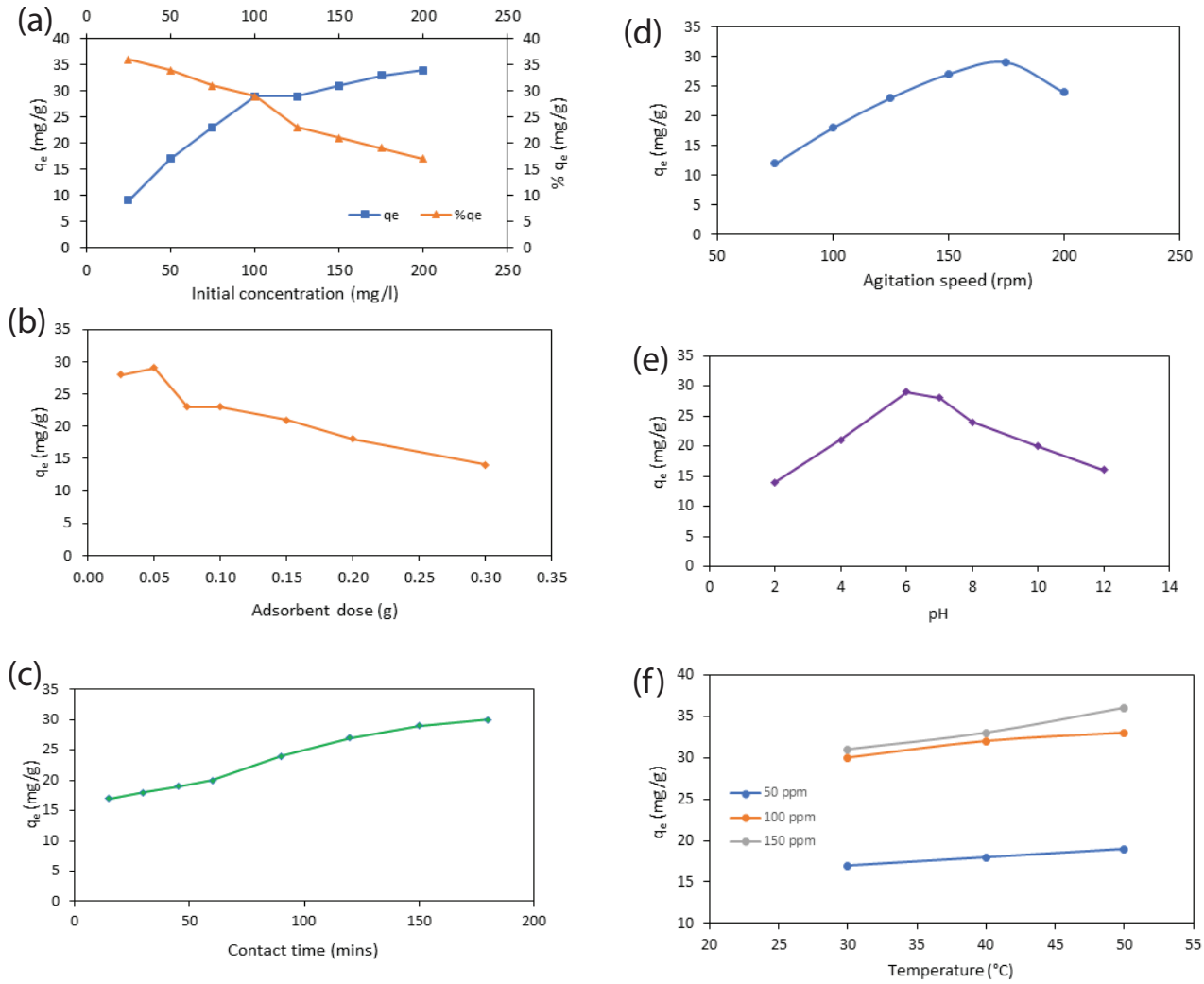

Fig. 8. (a) Effect of initial dye concentration q_e and % q_e; (b) effect of adsorbent dosage; (c) effect of contact time; (d) effect of speed of agitation; (e) effect of pH on adsorption and (f) effect of temperature with different dye concentration.

to 200 rpm to study the effect on maximum uptake of the dye by adsorbent. It was found that the adsorption capacity of adsorbent increased when the agitation speed increased from 75 to 175 rpm and thereafter decreased. Hence for all the experiments 165 rpm was chosen.

3.2.5. Effect of pH

The initial pH of the dye solution plays an important role in the adsorption process. It is likely to have an influence on the adsorption capacity, surface charge of the adsorbent and extent of ionization of the dye present in the solution. It is likely to influence the ionization/dissociation of the functional group(s) on the active sites of the adsorbent and solution chemistry of the dyes. In the present study, the effects of the initial pH of AV49 dye solution were examined with pH range of 2–12 and the results are presented in Fig. 8(e). The adsorption uptake was less at lower pH and increased with increase in pH and maximum adsorption efficiency was reached at pH 6.0 (q_e = 29.00 mg/g) and at neutral pH 7.0 (q_e = 28.0 mg/g) with initial dye concentration of 100 mg/L. This is in confirmation with the results of the point of zero charge which is found to be pH 7.20. At lower pH, the number of positive charged adsorbent surface sites increased probably due to the formation of $–OH_2^+$ on the cellulosic adsorbent matrix which increased the electrostatic repulsion between the positively charged dye molecules. At pH > 7 the decrease in adsorption efficiency may be due to possibility of formation of new species as it is observed in many of the triphenyl class of dyes.

3.2.6. Effect of temperature

Temperature is a significant parameter which has two major effects on the adsorption process. First, increasing temperature decreases the viscosity of the dye solution which accelerates the diffusion rate within the pores. Second, it alters the equilibrium capacity of the adsorbent and adsorbate. The studies were carried out at 30°, 40° and 50°C temperatures to make it easy for commercial application as the atmospheric temperature may not exceed more than 50°C in most of the places (Fig. 8(f)). A marginal increase in the

dye uptake capacity with increase in temperature may be due to increased mobility of the dye molecules and decrease in the retarding forces acting on the molecules [44].

3.2.7. Adsorption isotherm

The equilibrium relationship between the concentration of the liquid adsorbate and that of the adsorbent's surface at designed experimental conditions is described by the isotherm. In the present case, the relationship between adsorbent (NICSW) and adsorbate (AV49 dye) at equilibrium was examined. This is achieved by calculating the maximum adsorption capacity of the adsorbent through the application of well-established isotherm models namely, Langmuir, Freundlich, Temkin, Harkins–Jura, Jovanovic and Dubinin–Radushkevich.

According to Langmuir isotherm [45], adsorption occurs on a homogeneous surface where all sites are provided equal energy for adsorption. This applies for the entire monolayer of adsorption, where no transmigration of adsorbate takes place on the surface plane. The Q_m value of 45.4 mg/g obtained for this isotherm has not much deviation from the experimental value of q_e (29.00 mg/g), and R^2 of 0.979 obtained shows good fitting between the isotherm and experimental data (Fig. 9(a)). Hence the separation factor (R_L) plays an important role in Langmuir isotherm [46]. This is helpful in the verification as to whether the adsorption in the system belongs to any of these categories; that is unfavorable ($R_L > 1$), linear ($R_L = 1$), favorable ($0 < R_L < 1$), or irreversible ($R_L = 0$). In the present case, the dye concentration studied (25–200 mg/L), the values coming between 0.67 and 0.20 indicate favorable adsorption of the AV49 dye by NICSW. The decrease in R_L with increase in the initial concentration indicates that the adsorption is more favorable at higher concentrations. The values for maximum adsorption amount (Q_m), correlation coefficient (R^2), chi-square (χ^2) and other parameters for all the isotherms are shown in Tables 3 and 4.

Freundlich isotherm is an empirical equation. It is used for heterogeneous systems where there is interaction between the molecules adsorbed [47]. The heterogeneity factor n_f, indicates the nature of adsorption whether the adsorption is linear ($n_f = 1$), chemical process ($n_f < 1$), or a physical process ($n_f > 1$). The values of $1/n_f < 1$ and $1/n_f > 1$ indicate a normal Langmuir isotherm and cooperative adsorption. The $n_f = 2.262$ and $1/n_f = 0.442$ values show that process is physical and the normal Langmuir isotherm is favorable. The experimental data ($R^2 = 0.927$) fitted to the Freundlich isotherm is shown in Fig. 9(a).

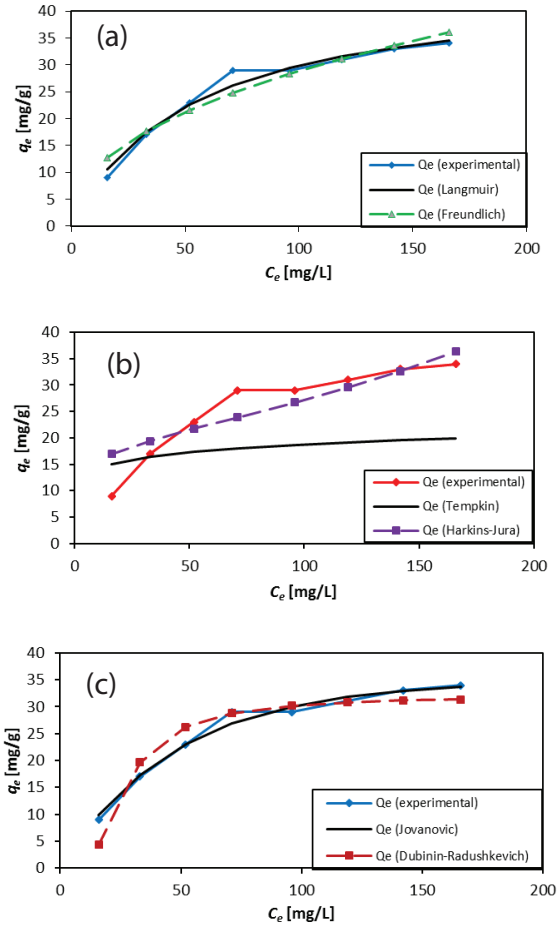

Fig. 9. (a) Fitting of adsorption data to Langmuir and Freundlich adsorption isotherms. (b) Fitting of adsorption data to Temkin and Harkins–Jura adsorption isotherms and (c) Fitting of adsorption data to Jovanovic and Dubinin–Radushkevich adsorption isotherms.

Table 3
Calculated isotherm parameters of AV49–NICSW system using different models

Langmuir		Freundlich		Temkin		Harkins–Jura		Jovanovic		Dubinin–Radushkevich	
Q_m	45.40	K_f	3.76	b_T	750	A_{hj}	1,122.62	Q_m	34.72	Q_s	31.99
K_S	0.0192	n_f	2.262	k_T	29.73	B_{hj}	4.77	K_J	2.09E-02	K_{ad}	8.59E-05

Table 4
Statistical parameters of AV49-NICSW system

Isotherms	Langmuir	Freundlich	Temkin	Harkins–Jura	Jovanovic	Dubinin–Radushkevich
SSE	12.0	40.1	260.3	109.1	7.4	51.6
χ^2	0.63	2.52	20.14	8.66	0.31	3.68
R^2	0.979	0.927	0.977	0.815	0.987	0.917

The interactions between adsorbent–adsorbate molecules are considered by Temkin isotherm (Fig. 9(b)). It presumes that for all molecules heat of adsorption decrease linearly instead at logarithmic scale when the layer is covered. It also presumes that the adsorption has a maximum uniform distribution of binding energy [48]. The high positive value of molecular interaction constant (b_T = 750) indicates that there is significant resistance to formation of multiple layers of adsorbate due to repulsion between similar molecules. The fit to experimental data (R^2 = 0.977) shows that the Temkin isotherm is less adequate to explain the adsorption of AV49 dye onto NICSW, as compared with the Langmuir isotherm.

The Harkins–Jura adsorption isotherm accounts to multilayer adsorption on a heterogeneous pore distribution [49,50]. According to the authors the adsorptive film is condensed type and its surface pressure is the difference between the bare surface and film covered surface tensions and is nothing but linear function of the area per molecule (Fig. 9(b)). However, very little information is available to extend the Harkins–Jura equation to the solution–solid systems. Our attempt to use this model for the adsorption of AV49 dye on NICSW has not yielded encouraging results.

The Jovanovic isotherm [51] describes a model that is very similar to that of Langmuir, it has Q_m = 34.72 mg/g considering a monolayer and no lateral interactions. Looking at the Q_m, χ^2 (0.31) and R^2 (0.987) values it could be concluded that Langmuir is a better fit (Fig. 9(c)).

Dubinin–Radushkevich isotherm is an empirical model and it is commonly applied to express adsorption mechanism in such cases where there is a Gaussian energy distribution on a heterogeneous surface [52]. This model distinguishes successfully the physical and chemical adsorption of metal ions. This model is typically temperature dependent. The fits of Dubinin–Radushkevich isotherm (R^2 = 0.917) is shown in Fig. 9(c).

Models used to understand the mechanism of adsorption are of mathematically higher order equations. The validity of data fitting cannot be confirmed by R^2 value alone because it is a statistical evaluation to be used with linear models only. Hence, χ^2 values are considered as they provide a better evaluation because the model data are similar to the experimental data. Thus, lower the value of χ^2 is the indication for better fit to the model, while, higher value represents variation in the experimental data. From the analysis of the isotherms and the understanding of the most important parameters (Q_m, R^2 and χ^2), the isotherms can be arranged according to their capacity to predict their efficiency in experimental behavior of AV49–NICSW system. With respect to χ^2 (analysis the models can be arranged in the order): Temkin > Harkins–Jura > Dubinin–Radushkevich > Freundlich > Langmuir > Jovanovic.

3.2.8. Adsorption kinetics

Kinetic models were studied in order to find out the potential rate-controlling steps involved in the process of adsorption. The concentrations of AV49 dye used were 50, 100 and 150 ppm for kinetic studies. Kinetic studies conducted at different temperatures (303, 313 and 323 K) reveal the change in adsorption rate at different temperature. The adsorption kinetic data were analyzed by non-linear analyses (MS Excel 2010) using such kinetic models as: pseudo-first-order [53], pseudo-second-order [54], intraparticle diffusion by Weber–Morris model [55], Dumwald–Wagner model [56] and film diffusion model [57]. The estimated parameters are shown in Tables 5 and 6.

Based on coefficients of determination (R^2) and chi-square values (χ^2), the pseudo-second-order model fitted better than pseudo-first-order with the experimental data at all initial AV49 dye concentrations (50, 100 and 150 ppm) at different temperature as shown in Figs. 10(a)–(c). The rate of adsorption which was very high initially slowed down gradually to become stagnant when it reached the maximum adsorption. The adsorption capacity (q_e) increased with increase in temperature. These results signify that the adsorption processes were not rate-limiting. The data also show that adsorption process occurred in multiple steps where the solute molecules move from the bulk solution to solid surface followed by diffusion of the solute molecules to the pores of the NICSW.

3.2.9. Adsorption thermodynamics

Energy and entropy are the main factors under consideration in the interaction process design. Gibbs free energy

Table 5
Experimentally determined and theoretically predicted parameters for absorption kinetics models – AV49–NICSW system

Initial concentration (ppm)	Temperature		Pseudo-first-order				Pseudo-second-order			
	(K)	$q_e$expt (mg/g)	Qepred (mg/g)	k_1	R^2	χ^2	Qepred (mg/g)	k_2	R^2	χ^2
50	303	17	12.11	2.12E-02	0.91	0.80	15.87	1.26E-03	0.93	0.54
	313	18	12.49	2.61E-02	0.88	0.93	15.73	1.74E-03	0.90	0.58
	323	19	14.67	2.42E-02	0.85	1.41	18.53	1.36E-03	0.87	0.95
100	303	30	21.24	2.95E-02	0.74	2.77	28.72	1.36E-03	0.78	1.84
	313	32	23.11	2.97E-02	0.76	2.72	29.06	1.23E-03	0.80	1.77
	323	33	24.31	3.60E-02	0.70	2.81	31.87	1.56E-03	0.78	1.71
150	303	31	24.40	2.60E-02	0.77	3.17	30.01	9.78E-04	0.79	2.19
	313	33	24.56	3.09E-02	0.74	2.94	31.86	1.19E-03	0.79	1.91
	323	36	26.77	3.37E-02	0.82	2.12	34.39	1.21E-03	0.87	1.18

Table 6
Calculated parameters of diffusion models of AV49–NICSW system

Initial Concentration (ppm)	Temperature (K)	Film diffusion model		Weber-Morris model		Dumwald-Wagner	
		R^1 (min^{-1})	R^2	k_{ist} (mg g^{-1} s$^{-0.5}$)	R^2	K (min^{-1})	R^2
50	303	0.0203	0.95	0.92	0.98	0.018	0.94
	313	0.0203	0.95	0.92	0.98	0.018	0.94
	323	0.0203	0.95	0.92	0.98	0.019	0.94
100	303	0.0215	0.91	1.47	0.98	0.020	0.89
	313	0.0216	0.90	1.47	0.97	0.020	0.88
	323	0.0253	0.89	1.59	0.95	0.023	0.88
150	303	0.0192	0.97	0.85	0.97	0.018	0.97
	313	0.0208	0.96	1.02	0.98	0.020	0.96
	323	0.0228	0.97	1.20	0.99	0.023	0.97

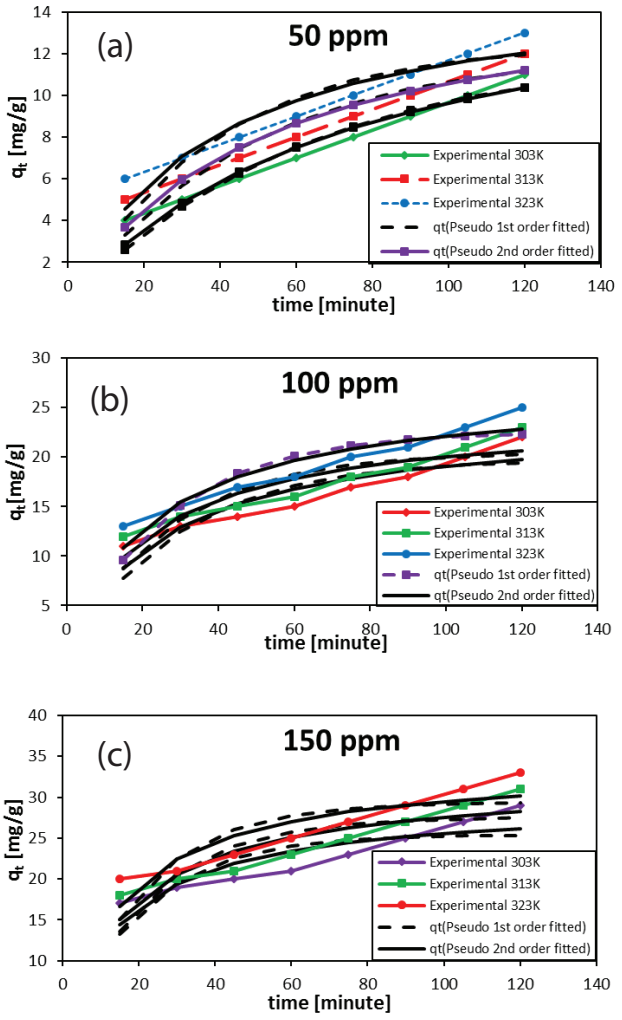

Fig. 10. (a) Kinetic model fits for 50 ppm initial concentration of AV49 dye on NICSW system at different temperatures, (b) kinetic model fits for 100 ppm initial concentration of AV49 dye on NICSW system at different temperature and (c) kinetic model fits for 150 ppm initial concentration of AV49 dye on NICSW system at different temperatures.

change ($\Delta G°$) indicates the extent of spontaneity of adsorption. When the free energy change ($\Delta G°$) of adsorption is negative, significant adsorption occurs. Changes pertaining to Gibbs free energy, entropy and enthalpy of adsorption could be arrived at by Van't Hoff and Gibbs–Helmholtz equations:

$$K_L = \frac{C_o}{C_e} \tag{4}$$

$$\Delta G° = -RT \ln K_L \tag{5}$$

$$\ln K_L = \frac{\Delta S°}{R} - \frac{\Delta H°}{RT} \tag{6}$$

where K_L is the thermodynamic equilibrium constant (L/mol) and T is the temperature (K). C_o and C_e are initial and equilibrium concentrations (mg/L) of dye in solution, respectively. $\Delta H°$ and $\Delta S°$ can be determined from the slope and the intercept of the Van't Hoff plots of ln (K_L) vs. 1/T and E_a can be determined from the slope and the intercept of the Van't Hoff plots of ln (K_2) vs. 1/T as shown in Figs. 11(a) and (b).

The thermodynamic parameter estimates are presented in Table 7. The positive $\Delta H°$ value suggests the endothermic nature of adsorption and the negative $\Delta G°$ values indicate the feasibility and spontaneity of the adsorption process. The $\Delta G°$ is negative for all studied temperatures indicating that the adsorption of AV49 dye onto NICSW would follow a spontaneous and favorable trend. The $\Delta G°$ value decreases with increase in temperature indicating increase in adsorption at higher temperatures. The positive value of $\Delta S°$ suggests good affinity of AV49 dye towards the adsorbent and increased randomness at the solid solution surface. The extremely low values of $\Delta H°$ suggest that the adsorption process is physical as the standard enthalpy change for chemical reaction is normally >200 kJ/mol. This has been further confirmed by activation energy values of the adsorption process at different initial concentrations (50, 100 and 150 ppm) which ranged from ~3.35 to 8.73 kJ/mol using the Arrhenius equation and the kinetic constant from the pseudo-second order model (Table 7).

3.2.10. Statistical optimization by fractional factorial experiment design

Six factors affecting the adsorption process were studied for their effects on the final adsorption capacity (q_e); these included adsorption time (A), process temperature (B), initial dye concentration (C), agitation speed (D) adsorbent dosage (E) and initial pH (F). A standard experiment design was set up with six factors at two levels with minimum and maximum values as shown in Table 1 for each independent factor. ANOVA (Table 8) was conducted based on the results obtained and significance of factors was decided at confidence level of 95% or with p-value of ≤0.05%. Among the factors A, B, C, D, E, AC, BC, A^2, C^2, D^2 and F^2 were highly significant. The goodness of fit for RSM model is evaluated with model F-value of 185.9 which was highly significant. Predicted R^2 value of 93.5 is very close with adjusted R^2 of 96.0%. High R^2 value of 96.5% with CV of 5.3% proves that model can be used to navigate the design space. The comparison graph for actual vs. predicted values (Fig. 12) indicate a strong relationship between the experiment and predicted responses. A final quadratic equation based on regression analysis is shown below:

$$q_e = 20.3 + 6.5*A + 2.2*B + 0.9*C + 6.4*D - 6.1*E + 0.1*F + 0.2*AB + 2.1*AC + 1.6*BC - 2.4*A^2 - 0.03*B^2 - 18.5*C^2 - 7.2*D^2 - 0.7*E^2 - 11.2*F^2 \quad (7)$$

The optimal value of each variable was determined by maximizing the second-order polynomial equation along with interaction arrived at by multiple regression analysis which is based on FFED. Maximum adsorption value as arrived at by statistical optimization was 39.00 mg/g. The optimized conditions were pH 7, biosorbent dosage 0.600 g/L and an initial dye concentration 155 mg/L, adsorption time 180 min and orbital shaking of 161 rpm at 50°C temperature.

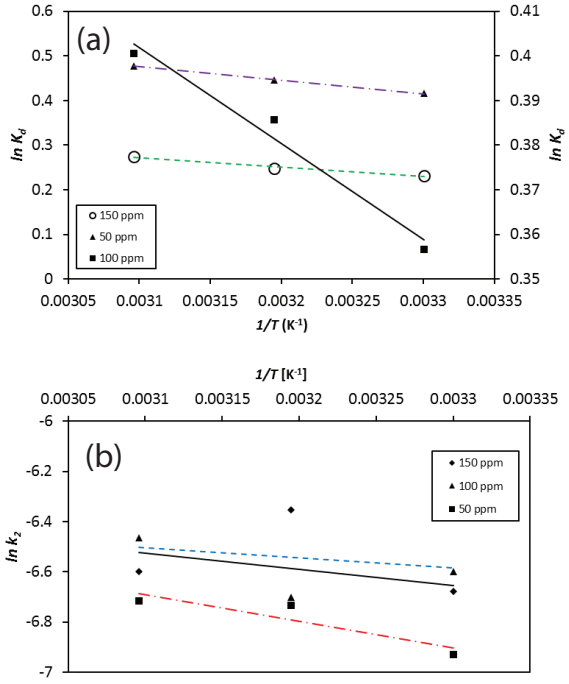

Fig. 11. (a) Plot of thermodynamic equilibrium constant vs. 1/T to determine the enthalpy and Gibbs free energy of the process and (b) plot of pseudo-second-order kinetic constant vs. 1/T to determine the activation energy of the process.

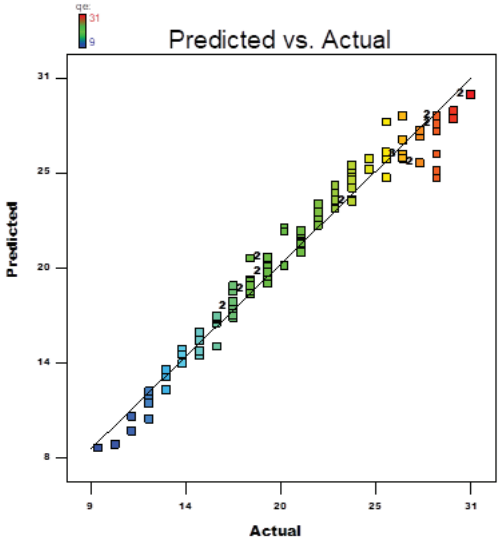

Fig. 12. Comparison graph for predicted vs. actual values of absorbance of AV49 dye on NICSW using RSM study.

Table 7
Thermodynamic parameters of AV49–NICSW system

Initial concentration (ppm)	Temperature (K)	$\Delta G°$ (kJ/mol)	$\Delta S°$ (J/mol/K)	$\Delta H°$ (kJ/mol)	ln A	E_a (kJ/mol)
150	303	–0.58	7.66	1.74	–5.25	3.35
	313	–0.65				
	323	–0.74				
100	303	–0.90	8.88	1.79	–4.50	5.43
	313	–1.00				
	323	–1.08				
50	303	–1.05	11.84	2.54	–3.43	8.73
	313	–1.16				
	323	–1.28				

Table 8
ANOVA of AV49–NICSW system

Source	Sum of squares	Degree of freedom	Mean square	*F*-value	*p*-value
Model	3,454.1	15	230.3	185.9	<0.0001**
A	660.8	1	660.8	533.4	<0.0001**
B	188.4	1	188.4	152.1	<0.0001**
C	12.0	1	12.0	9.7	<0.0001**
D	183.0	1	183.0	147.7	<0.0001**
E	149.1	1	149.1	120.4	<0.0001**
F	0.1	1	0.1	0.05	0.8304
AB	0.6	1	0.6	0.5	0.4776
AC	30.2	1	30.2	24.4	<0.0001**
BC	26.4	1	26.4	21.3	<0.0001**
A^2	47.7	1	47.7	38.5	<0.0001**
B^2	0.01	1	0.0	0.0	0.9239
C^2	1,325.5	1	1,325.5	1,070.0	<0.0001**
D^2	51.4	1	51.4	41.5	<0.0001**
E^2	0.8	1	0.8	0.7	0.4214
F^2	234.5	1	234.5	189.3	<0.0001**
Residual	125.1	101	1.2		
Total	3,579.197	116			

** Strongly significant $p \leq 0.01$
Moderately significant $0.01 < p \leq 0.05$
Suggestive significant $0.05 < p < 0.10$
Non-significant $p > 0.10$.

The 3D response surface plots and contour plots as a function of two independent variables. These helped in determining the effects of interaction behavior between two factors keeping other parameters at a fixed value (in this case the optimum value).

Statistical optimization of process, in a determined range of values of parameter, allows both for calculating the optimal condition, and determination of the process conditions on biosorption. Maximum concentration is nearly 113.00 mg/L beyond which any increase in concentration shows negative effect but increase of time alone has positive effect. The regression coefficient values are the indications of the effect of parameters on adsorption capacity. If the values are positive they indicate incremental effect, as for example, the increase in time (*A*) significantly increases the adsorption capacity. In contrast, a negative value signifies detrimental effect, as evident from absorbent dosage (*E*), where the increase in dosage lowers the adsorption capacity of adsorbent. Thus, effects of two parameters simultaneously by biosorption are presented in the surface and contour plots (Figs. 13(a)–(c)).

3.2.11. Adsorption mechanism of AV49 dye onto NICSW

The process of adsorption of the dye onto the adsorbent is governed by mass transfer phenomena. According to the experimental findings and statistical optimization of process parameters, the mechanism of adsorption involves the following steps:

- Mass transfer of AV49 dye from bulk solution onto the adsorbent is fast at the initial stages till monolayer is formed.
- Mechanical agitation has profound influence on mass transfer.
- Diffusion is a slow process.
- The hydrogen bonds are formed.
- The influence of weak Van der Waals forces plays a major role.
- Electrostatic forces of attraction between the cation dye is due to the process of  and negative charge $-OH^-$ group of NICSW.

On the basis of the above physical model, the interaction of adsorbent and adsorbate is drawn as shown in Fig. 14. Similar physical modeling is already reported for malachite green dye and conch shell powder [58].

4. Application of proposed method to textile industrial effluent

Different processes employed in textile industry generate waste water with varied composition containing, large amounts of suspended solids, highly fluctuating pH, variable temperature, intense color and COD concentration [59]. Therefore, it is difficult to identify a specific dye in industrial effluent due to matrix effect [60]. A simple procedure was developed to compare the remediation of AV49 dye in water as also in textile industrial effluent.

4.1. Textile industrial effluent

Effluent samples were collected from a local textile industry which operates in two shifts. Six random textile industrial effluent (TIE) samples were collected in 10-L polyethylene containers from the pipe delivering end where

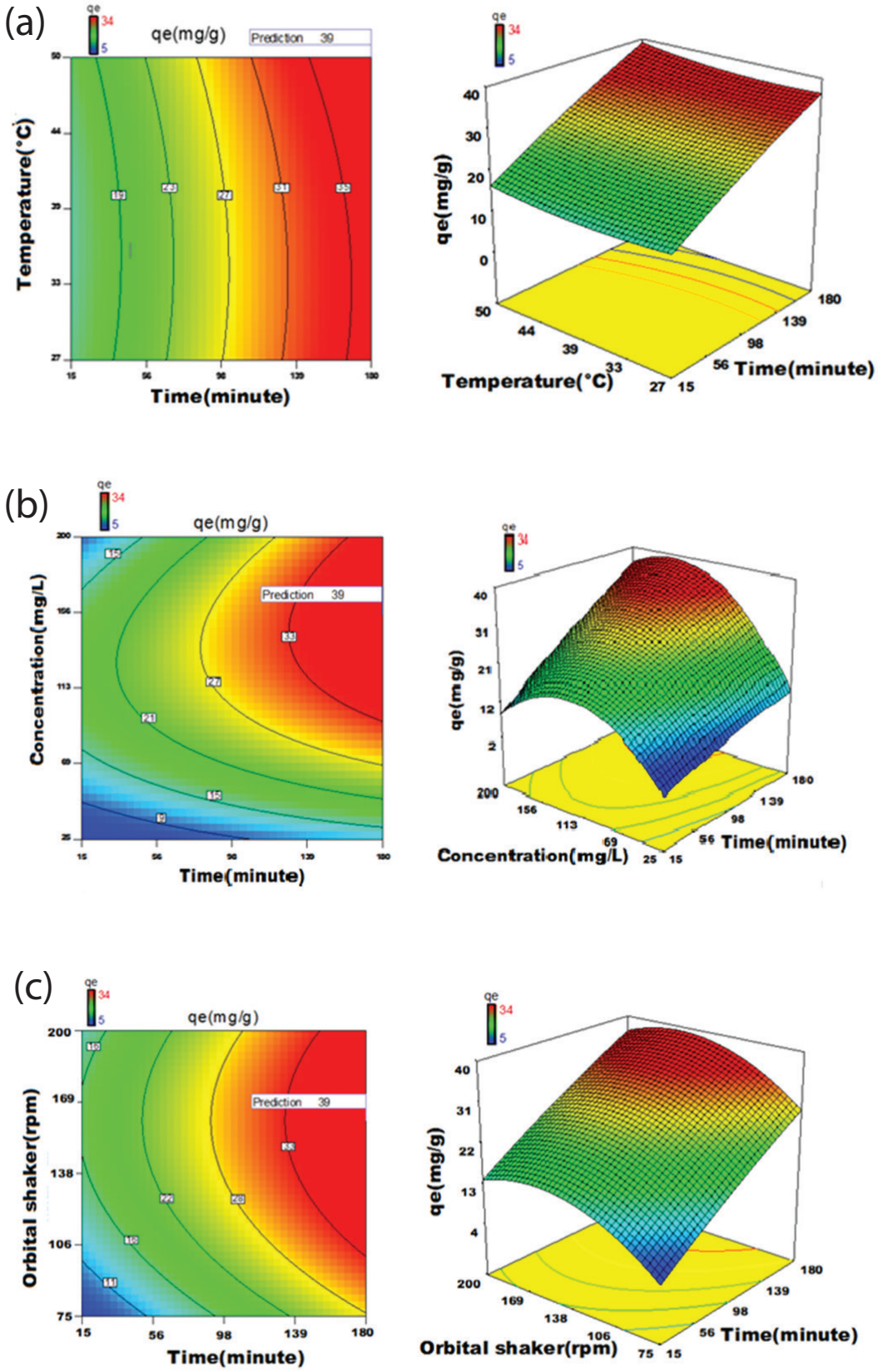

Fig. 13. (a) Contour plot and 3D surface plot showing the variation of adsorption capacity with time and temperature, (b) contour plot and 3D surface plot showing the variation of adsorption capacity with time and concentration and (c) contour plot and 3D surface plot showing the variation of adsorption capacity with temperature and concentration.

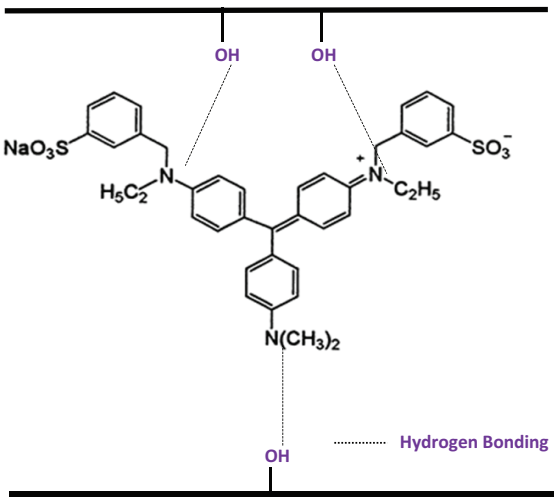

Fig. 14. Schematic representation of hydrogen bonding between adsorbent and adsorbate.

the effluent enters inside the treatment plant. Among the six samples, three were collected from first and second shifts consecutively on three working days. All textile industrial effluent samples collected were transferred to a 100-L barrel and stirred manually to get uniform concentration. The resulting solution was used as control TIE sample for analyses. Sampling, preparation and preservation methods followed while collecting the effluent samples from the industries were in accordance with standard methods [61].

4.2. Preparation of AV49 dye in distilled water

2 g of AV49 dye were transferred to a 2-L standard flask. The dye was dissolved in distilled water and the solution was made up to the mark. The resulting solution was stirred to uniform concentration (Solution 1).

4.3. Preparation of AV49 dye in textile industrial effluent

2 g of AV49 dye were transferred to a 2-L standard flask. The dye was dissolved in TIE and the solution was made up to the mark with TIE. The resulting solution was stirred to uniform concentration (Solution 2).

4.4. Blank experiment

500 mL of distilled water were transferred to a 1-L conical flask containing 5-cm Teflon-coated magnetic bar. 5 g of NICSW were added and the solution stirred at about 700 rpm for 15 min using a magnetic stirrer. The solution was filtered using No. 42 Whatman filter paper and the filtrate solution was compared with the solution obtained after remediation of dye-loaded TIE.

4.5. Procedures

4.5.1. Measurement of the absorbance of stock solutions

An aliquot solution of TIE was filtered through Büchner funnel apparatus using No. 42 Whatman filter paper and the absorbance of the filtrate was measured using UV–Vis Spectrophotometer (PerkinElmer-Lambda 25, USA) with a maximum absorbance scale of 3.0. All absorbance values were measured within this range. However, in case of concentrated solutions, the absorbance was measured after appropriate dilution and the resultant absorbance was multiplied by the dilution factor to get the absorbance of concentrated solution. This procedure was repeated to measure the absorbance of Solution 1 and Solution 2.

Step 1: 500 mL of Solution 1 were transferred to a 1-L conical flask. 5 g of NICSW were added to the conical flask and the solution was agitated at about 700 rpm using magnetic stirrer. At the end of 15 min, the agitation was stopped and solution was filtered through No. 42 Whatman filter paper using Büchner funnel apparatus. If the filtrate is not clear, the filtration was repeated and absorbance recorded.

Step 2: The dye-adsorbed NICSW on the filter paper of Step 1 was carefully transferred from a Büchner funnel to a watch glass and kept in an oven at 60°C for 24 h for drying. The dried powder was scrapped using spatula and transferred to a watch glass.

Step 3: Second portion of 5 g NICSW was added to the conical flask containing filtrate solution from Step 1 and agitation was continued on a magnetic stirrer at about 700 rpm for 15 min. At the end of 15 min, the agitation was stopped and solution was filtered through No. 42 Whatman filter paper using Büchner funnel apparatus. If the filtrate is not clear, the filtration was repeated and absorbance recorded.

Step 4: The dye-adsorbed NICSW on the filter paper of the Step 3 was carefully transferred from a Büchner funnel to a watch glass and kept in an oven at 60°C for 24 h for drying. The dried powder was scraped using spatula and transferred to a watch glass.

Step 5: Third portion of 5 g NICSW was added to the conical flask containing filtrate solution from Step 3 and agitation was continued on a magnetic stirrer at about 700 rpm for 15 min. At the end of 15 min, the agitation was stopped and solution was filtered through No. 42 Whatman filter paper using Büchner funnel apparatus. If the filtrate is not clear, the filtration was repeated and absorbance recorded.

Step 6: The dye-adsorbed NICSW on the filter paper of the Step 5 was carefully transferred from a Büchner funnel to a watch glass and kept in an oven at 60°C for 24 h for drying. The dried powder was scrapped using spatula and transferred to a watch glass.

Step 7: Fourth portion of 5 g NICSW was added to the conical flask containing filtrate solution from Step 5 and agitation was continued on a magnetic stirrer at about 700 rpm for 15 min. At the end of 15 min, the agitation was stopped and solution was filtered through No. 42 Whatman filter paper using Büchner funnel apparatus. If the filtrate is not clear, the filtration was repeated and absorbance recorded.

Step 8: The dye-adsorbed NICSW on the filter paper of the Step 7 was carefully transferred from a Büchner funnel to a watch glass and kept in an oven at 60°C for 24 h for drying. The dried powder was scrapped using spatula and transferred to a watch glass.

Step 9: Steps 1 to 8 were repeated with Solution 2.

The powder and filtrate solutions after the adsorption of constituents of Solution 2 on NICSW are shown in Figs. 15(a) and (b).

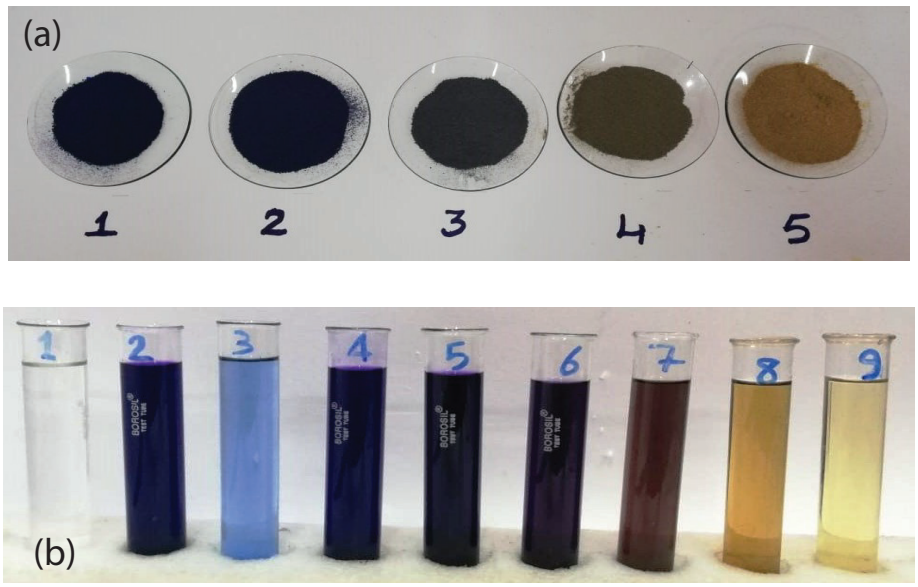

Fig. 15. (a) Powders 1 to 4: Fresh samples of NICSW added to AV49–TIE solution after every 15 min, filtered and the residue dried in oven. Sample 5: NICSW; (b) 1. Distilled water; 2. AV49 dye in distilled water; 3. TIE; 4. AV49 dye in TIE; Filtrate after adsorption of dye on NICSW after 5. 15 min; 6. 30 min; 7. 45 min; 8. 60 min; 9. Filtrate of NICSW in distilled water.

Preliminary trial revealed that better results could be obtained by scaling up to two-orders of the adsorbent and the adsorbate and to one order of the volume of the solution. In an interesting observation, Solution 2 showed about 20% decrease in absorbance compared with Solution 1. This may be due to the absorbance of the dye by various undefined constituents present in TIE. Also, it was observed that additional fresh samples of the adsorbent after every 15 min enhanced the efficiency of removal of the dye from TIE. The recovery of the dye and allied substances from Solution 2 to an extent of 51%, 85%, 92% and 96% after 15, 30, 45 and 60 min, respectively, was observed. This observation is in accordance with the kinetic results according to which the solute adsorbs quickly onto the surface of the particles forming a film which then gets retarded further diffusion thereby bringing change in absorption rates.

The experiment was scaled up to 10, 20, and 50 g of NICSW using 1, 2, and 5 L of Solution 2 taken in polyethylene beakers. The solutions were vigorously stirred using a magnetic stirrer and the procedure repeated as indicated earlier and the results obtained were almost uniform. All experiments were carried out in triplicate and the mean of three replications are reported. The coefficients of variance of all results did not exceed ±2% error.

In brief, an attempt to scale up of the experiment by about three orders of its initial set up has given promising results. The industrial effluents may have many variables that may not be exactly interpreted from the initial data. This is always a serious limitation in such studies. The outcome could be pin pointedly focused by resorting to much larger pilot scale study. However, the fact that the limitations of scale have been recognized, and that the enhanced scale experimental data will definitely continue to show promise and reliability of the process, which in fact may be sufficient to prove that the principles of the method when operated on a larger scale in industries will definitely prove its usefulness. It is envisaged that the treated textile industrial effluent can be used for agricultural purpose. However, more investigations are required for the possible use of water for human consumption.

4.5.2. Regeneration of the adsorbent and cost analysis

Regeneration of dye-loaded NICSW enables the re-use of the biomass, and recovery and/or containment of adsorbed AV49 dye material. However, it is not a feasible proposition as the cost of the process and the solvents used will be far higher than the cost of the sorbent (NICSW) used in the processes. Besides, it will enhance the E-factor which is highly undesirable as the planet earth cannot afford the load of environmental toxicant as it will almost lead to a disaster. In view of increased stringencies imposed on pollution, a novel approach has been developed to use the dye-adsorbed biosorbent generated waste to be used as a filler material for the fabrication of thermosets and thermoplastics. The work in this direction is in progress in our research laboratory [32,35].

5. Conclusion

High costs of adsorbents used in remediation of dyes associated with stringent environmental considerations have led to resurgence of interest to identify low-cost adsorbents derived from renewable resources. In this context, the advantages of using nutraceutical industrial waste as the source of new adsorbents is primarily due to their high abundance, low-cost and as renewable sources. Consequently, the first-ever study on the use of chillies stalk, a waste which has no feed, fuel or fertilizer value assumes paramount importance. The adsorption interactions between nutraceutical industrial chillies stalk waste as adsorbent and acid violet 49 dye have been investigated by six two-parameter models and the result gave 29.00 mg/g adsorption rate. Kinetic and thermodynamic

studies have established that the process of adsorption is a physical phenomenon and follows second-order kinetics. Besides, the research work in progress at our school to utilize the dye-adsorbed adsorbent as filler material is going to be a sustainable proposition.

Symbols

n_F	—	Heterogeneity factor
q_e	—	Adsorption capacity, mg/L
Q_m	—	Maximum adsorption capacity, mg/g
q_t	—	Adsorption capacity at time t, mg/L
R^2	—	Correlation coefficient
R_L	—	Separation factor
χ^2	—	Chi-squared
AV49	—	Acid Violet 49 dye
BET	—	Brunauer–Emmett–Teller
EDS	—	Energy dispersive X-ray spectroscopy
FTIR	—	Fourier transform infrared spectroscopy
NICSW	—	Nutraceutical industrial chillies stalk waste
NIW	—	Nutraceutical industrial waste
SEM	—	Scanning electron microscopy
SSE	—	Sum of square errors

References

[1] R. Geetha, K. Selvarani, A study of chilli production and export from India, IJARIIE, 3 (2017) 205-210.
[2] http://www.fao.org/faostat/en/#home (Accessed on 31 July 2018).
[3] www.worstpolluted.org/2016-report.html (Accessed on 31 July 2018).
[4] U. Filipkowska, E. Klimiuk, S. Grabowski, E. Siedlecka, Adsorption of reactive dyes by modified chitin from aqueous solutions, Polish J. Environ. Stud., 11 (2002) 315–323.
[5] K. Kadirvelu, M. Kavipriya, C. Karthika, M. Radhika, N. Vennilamani, S. Pattabhi, Utilization of various agricultural wastes for activated carbon preparation and application for the removal of dyes and metal ions from aqueous solutions, Bioresour. Technol. 87 (2003) 129–132.
[6] S. Patil, V. Deshmukh, S. Renukdas, N. Patel, Kinetics of adsorption of crystal violet from aqueous solutions using different natural materials, Int. J. Environ. Sci., 1 (2011) 1116.
[7] Y.C. Wong, Y.S. Szeto, W.H. Cheung, G. McKay, Adsorption of acid dyes on chitosan—equilibrium isotherm analyses, Process. Biochem., 39 (2004) 695–704.
[8] W. Przystaś, E. Zabłocka-Godlewska, E. Grabińska-Sota, Biological removal of azo and triphenylmethane dyes and toxicity of process by-products, Water Air Soil Pollut., 223 (2012) 1581–1592.
[9] N.S. Maurya, A.K. Mittal, Biosorptive uptake of cationic dyes from aqueous phase using immobilised dead macro fungal biomass, Int. J. Environ. Technol. Manage., 14 (2011) 282–293.
[10] A. Jasińska, S. Różalska, P. Bernat, K. Paraszkiewicz, J. Długoński, Malachite green decolorization by non-basidiomycete filamentous fungi of *Penicillium pinophilum* and *Myrothecium roridum*, Int. Biodeterior. Biodegrad., 73 (2012) 33–40.
[11] G.Y. Lv, J.H. Cheng, X.Y. Chen, Z.F. Zhang, L.F. Fan, Biological decolorization of malachite green by *Deinococcus radiodurans* R1., Bioresour. Technol., 144 (2013) 275–280.
[12] J. Cheriaa, M. Khaireddine, M. Rouabhia, A. Bakhrouf, Removal of triphenylmethane dyes by bacterial consortium, Sci. World. J., 2012 (2012) 1–9.
[13] R. Rajeshkannan, N. Rajamohan, M. Rajasimman, Removal of malachite green from aqueous solution by sorption on hydrilla verticillata biomass using response surface methodology, Front. Chem. Eng. China, 3 (2009) 146–154.
[14] A.B. Albadarin, M.N. Collins, M. Naushad, S. Shirazian, G. Walker, C. Mangwandi, Activated lignin-chitosan extruded blends for efficient adsorption of methylene blue, Chem. Eng. J., 307 (2017) 264–272.
[15] A.A. Alqadami, M. Naushad, M.A. Abdalla, M.R. Khan, Z.A. Alothman, Adsorptive removal of toxic dye using Fe_3O_4–TSC nanocomposite: equilibrium, kinetic, and thermodynamic studies, J. Chem. Eng. Data, 61 (2016) 3806–3813.
[16] G. Sharma, M. Naushad, A. Kumar, S. Rana, S. Sharma, A. Bhatnagar, M.R. Khan, Efficient removal of coomassie brilliant blue R-250 dye using starch/poly (alginic acid-cl-acrylamide) nanohydrogel, Process. Saf. Environ., 109 (2017) 301–310.
[17] T.A. Khan, E.A. Khan, Adsorptive uptake of basic dyes from aqueous solution by novel brown linseed deoiled cake activated carbon: equilibrium isotherms and dynamics, J. Environ. Chem. Eng., 4 (2016) 3084–3095.
[18] T.A. Khan, R. Rahman, E.A. Khan, Adsorption of malachite green and methyl orange onto waste tyre activated carbon using batch and fixed-bed techniques: isotherm and kinetics modeling, Modeling Earth Syst. Environ., 3 (2017) 38.
[19] M.A.A. Zaini, L.M. Salleh, M. Azizi, C. Yunus, M. Naushad, Potassium hydroxide-treated palm kernel shell sorbents for the efficient removal of methyl violet dye, Desal. Wat. Treat., 84 (2017) 262–270.
[20] G. Sharma, A. Kumar, M. Naushad, A. Kumar, H. Ala'a, P. Dhiman, M.R. Khan, Photoremediation of toxic dye from aqueous environment using monometallic and bimetallic quantum dots based nanocomposites, J. Clean. Prod., 172 (2018) 2919–2930.
[21] T.A. Khan, A.A. Mukhlif, E.A. Khan, Uptake of Cu^{2+} and Zn^{2+} from simulated wastewater using muskmelon peel biochar: isotherm and kinetic studies, Egypt, J. Basic. Appl. Sci., 4 (2017) 236–248.
[22] O. Moumeni, O. Hamdaoui, Intensification of sonochemical degradation of malachite green by bromide ions, Ultrason. Sonochem., 19 (2012) 404–409.
[23] L. Fan, Y. Zhou, W. Yang, G. Chen, F. Yang, Electrochemical degradation of aqueous solution of Amaranth azo dye on ACF under potentiostatic model, Dyes. Pigm., 76 (2008) 440–446.
[24] M.H. Baek, C.O. Ijagbemi, D.S. Kim, Spectroscopic studies on the oxidative decomposition of Malachite Green using ozone, J. Environ. Sci. Health A, 45 (2010) 630–636.
[25] C.G. Jerome, J.G. Theodore, F. Elizabeth, The Millennium Project, 4421 Garrison St., NW, Washington DC, 2014.
[26] M. Naushad, Z. Abdullah ALOthman, M. Rabiul Awual, S.M. Alfadul, T. Ahamad, Adsorption of rose Bengal dye from aqueous solution by amberlite Ira-938 resin: kinetics, isotherms, and thermodynamic studies, Desal. Wat. Treat., 57 (2016) 13527–13533.
[27] T.A. Khan, M. Nazir, Enhanced adsorptive removal of a model acid dye bromothymol blue from aqueous solution using magnetic chitosan bamboo sawdust composite: batch and column studies, Environ. Prog. Sustain. Energy, 34 (2015) 1444–1454.
[28] E.A. Khan, T.A. Khan, Adsorption of methyl red on activated carbon derived from custard apple (*Annona squamosa*) fruit shell: equilibrium isotherm and kinetic studies, J. Mol. Liq., 249 (2018) 1195–1211.
[29] T.A. Khan, S. Sharma, E.A. Khan, A.A. Mukhlif, Removal of congo red and basic violet 1 by chir pine (*Pinus roxburghii*) sawdust, a saw mill waste: batch and column studies, Toxicol. Environ. Chem., 96 (2014) 555–568.
[30] T.A. Khan, M. Nazir, E.A. Khan, Magnetically modified multiwalled carbon nanotubes for the adsorption of bismarck brown R and Cd (II) from aqueous solution: batch and column studies, Desal. Wat. Treat., 57 (2016) 19374–19390.
[31] T.A. Khan, M. Nazir, E.A. Khan, U. Riaz, Multiwalled carbon nanotube–polyurethane (MWCNT/PU) composite adsorbent for safranin T and Pb (II) removal from aqueous solution: batch and fixed-bed studies, J. Mol. Liq., 212 (2015) 467–479.
[32] S.N. Taqui, R. Yahya, A. Hassan, N. Nayak, A.A. Syed, Development of sustainable dye adsorption system using nutraceutical industrial fennel seed spent—studies using Congo red dye, Int. J. Phytorem., 19 (2017) 686–694.
[33] R. Sulthana, S.N. Taqui, F. Zameer, S.U. Taqui, A.A. Syed, Adsorption of ethidium bromide from aqueous solution on

to nutraceutical industrial fennel seed spent: kinetics and thermodynamics modeling studies, Int. J. Phytorem., 20 (2018) 1075–1086.
[34] P.K. Papegowda, A.A. Syed, Isotherm, kinetic and thermodynamic studies on the removal of methylene blue dye from aqueous solution using saw palmetto spent, Int. J. Environ. Res., 11 (2017) 91–98.
[35] S.N. Taqui, R. Yahya, A. Hassan, N. Nayak, A.A. Syed, A novel sustainable design to develop polypropylene and unsaturated polyester resin polymer composites from waste of major polluting industries and investigation on their physicomechanical and wear properties, Polym. Compos., 40 (2018) 1142–1157.
[36] S. Pashaei, Siddaramaiah, A.A. Syed, Investigation on mechanical, thermal and morphological behaviors of turmeric spent incorporated vinyl ester green composites, Polym. Plast. Technol. Eng., 50 (2011) 1187–1198.
[37] M.A. Syed, A.A. Syed, Development of green thermoplastic composites from Centella spent and study of its physicomechanical, tribological, and morphological characteristics, J. Thermoplast. Compos. Mat., 29 (2016) 1297–1311.
[38] M.A. Syed, A.A. Syed, Investigation on physicomechanical and wear properties of new green thermoplastic composites, Polym. Compos., 37 (2016) 2306–2312.
[39] M.A. Syed, A.A. Syed, Development of a new inexpensive green thermoplastic composite and evaluation of its physico-mechanical and wear properties, Mater. Des., 36 (2012) 421–427.
[40] M.A. Syed, S. Akhtar, A.A. Syed, Studies on the physic mechanical, thermal, and morphological behaviors of high density polyethylene/coleus spent green composites, J. Appl. Polym. Sci., 119 (2011) 1889–1895.
[41] M.A. Syed, B. Ramaraj, S. Akhtar, A.A. Syed, Development of environmentally friendly high density polyethylene and turmeric spent composites: physicomechanical, thermal, and morphological studies, J. Appl. Polym. Sci., 118 (2010) 1204–1210.
[42] M.A. Syed, Siddaramaiah, R.T. Syed, A.A. Syed, Investigation on physico-mechanical properties, water, thermal and chemical ageing of unsaturated polyester/turmeric spent composites, Polym. Plast. Technol. Eng., 49 (2010) 555–559.
[43] M.A. Syed, Siddaramaiah, B. Suresha, A.A. Syed, Mechanical and abrasive wear behaviour of coleus spent filled unsaturated polyester/polymethyl methacrylate semi interpenetrating polymer network composites, J. Compos. Mater., 43 (2009) 2387–2400.
[44] S. Chowdhury, P. Das, Utilization of a domestic waste—eggshells for removal of hazardous malachite green from aqueous solutions, Environ. Prog. Sustain. Energy, 31 (2012) 415–425.
[45] I. Langmuir, The constitution and fundamental properties of solids and liquids, J. Am. Chem. Soc., 38 (1916) 2221–2295.
[46] T.W. Webber, R.K. Chakkravorti, Pore and solid diffusion models for fixed-bed adsorbers, AlChE J., 20 (1974) 228–238.
[47] H.M.F. Freundlich, Over the adsorption in solution, J. Phys. Chem. 57 (1906) 385–471.
[48] M.I. Tempkin, V. Pyzhev, Kinetics of ammonia synthesis on promoted iron catalyst, Acta. Phys. Chim. USSR, 12 (1940) 327.
[49] W.D. Harkins, G. Jura, Surfaces of solids. XIII. A vapor adsorption method for the determination of the area of a solid without the assumption of a molecular area, and the areas occupied by nitrogen and other molecules on the surface of a solid, J. Am. Chem. Soc., 66 (1944) 1366–1373.
[50] W.D. Harkins, G. Jura, An adsorption method for the determination of the area of a solid without the assumption of a molecular area, and the area occupied by nitrogen molecules on the surfaces of solids, J. Chem. Phys., 11 (1943) 431–432.
[51] D.S. Jovanovic, Physical adsorption of gases, Colloid. Polym. Sci., 235 (1969) 1203–1213.
[52] M.M. Dubinin, The equation of the characteristic curve of activated charcoal, In Dokl. Akad. Nauk. SSSR, 55 (1947) 327–329.
[53] S. Lagergren, About the theory of so-called adsorption of soluble substances, K. Sven. Vetenskapsakad. Handl., 24 (1898) 1–39.
[54] Y.S. Ho, G. McKay, Sorption of dye from aqueous solution by peat, Chem. Eng. J., 70 (1998) 115–124.
[55] M. Alkan, Ö. Demirbaş, M. Doğan, Adsorption kinetics and thermodynamics of an anionic dye onto sepiolite, Microporous Mesoporous Mater., 101 (2007) 388–396.
[56] H.L. Wang, J.L. Chen, Z.C. Zhai, Study on thermodynamics and kinetics of adsorption of p-toluidine from aqueous solution by hypercrosslinked polymeric adsorbents, Environ. Chem., 23 (2004) 188–192.
[57] G.E. Boyd, A.W. Adamson, L.S. Myers Jr, The exchange adsorption of ions from aqueous solutions by organic zeolites. II. Kinetics, J. Am. Chem. Soc., 69 (1947) 2836–2848.
[58] S. Chowdhury, P. Das, Mechanistic, kinetic, and thermodynamic evaluation of adsorption of hazardous malachite green onto conch shell powder, Sep. Sci. Technol., 46 (2011) 1966–1976.
[59] P. Kumar, B. Prasad, I.M. Mishra, S. Chand, Catalytic thermal treatment of desizing wastewaters, J. Hazard. Mater., 149 (2007) 26–34.
[60] A.M. Talarposhti, T. Donnelly, G.K. Anderson, Colour removal from a simulated dye wastewater using a two-phase anaerobic packed bed reactor, Water Res., 35 (2001) 425–432.
[61] Standard Methods for the Examination of Water and Wastewater, 20th ed., American Public Health Association, Washington DC, 2002.

Supplementary figures

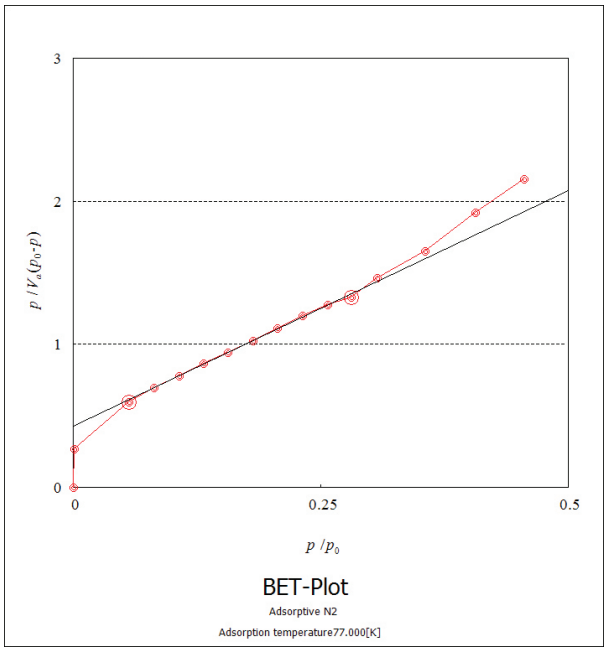

Fig. S1. BET plot of NICSW.

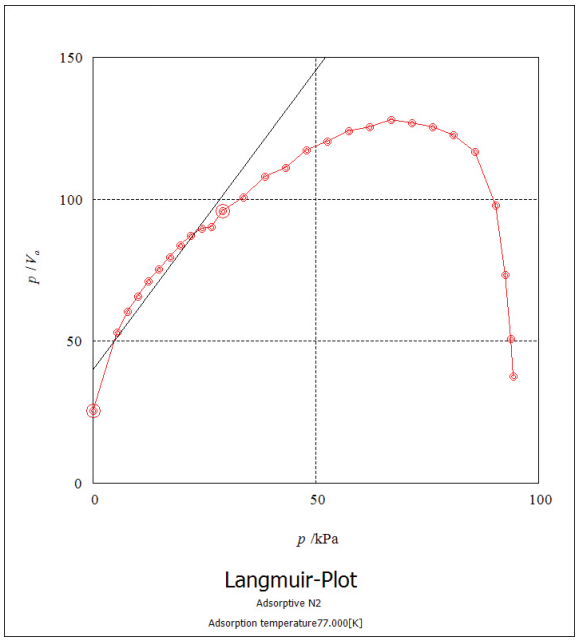

Fig. S2. Langmuir plot of NICSW.

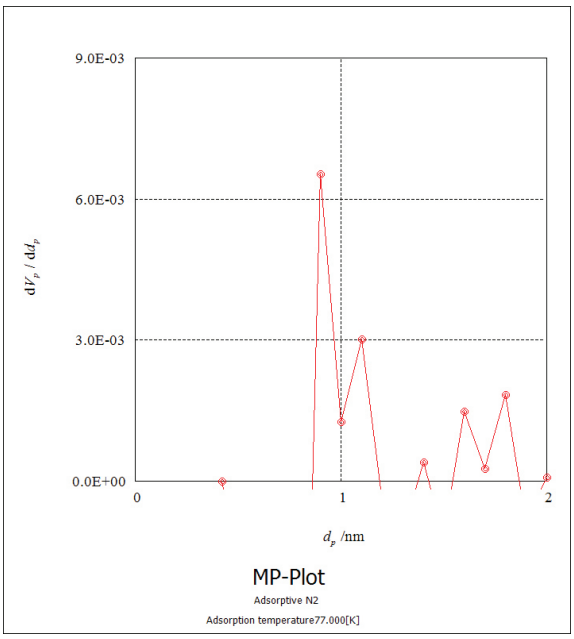

Fig. S3. MP plot of NICSW.

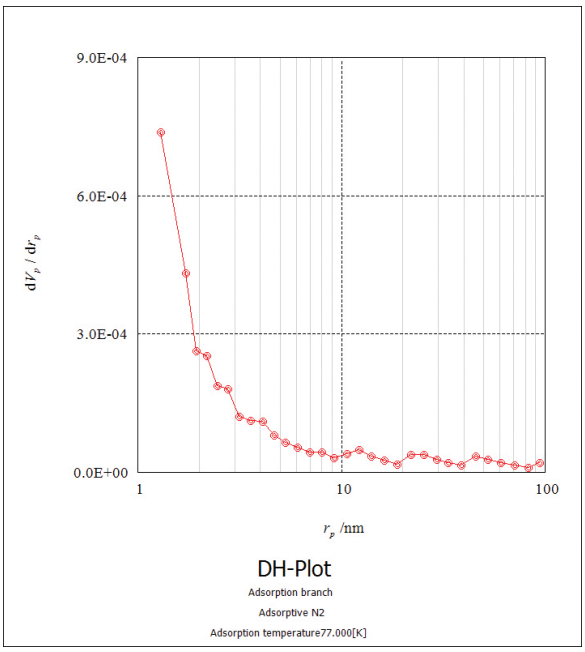

Fig. S5. DH plot of NICSW.

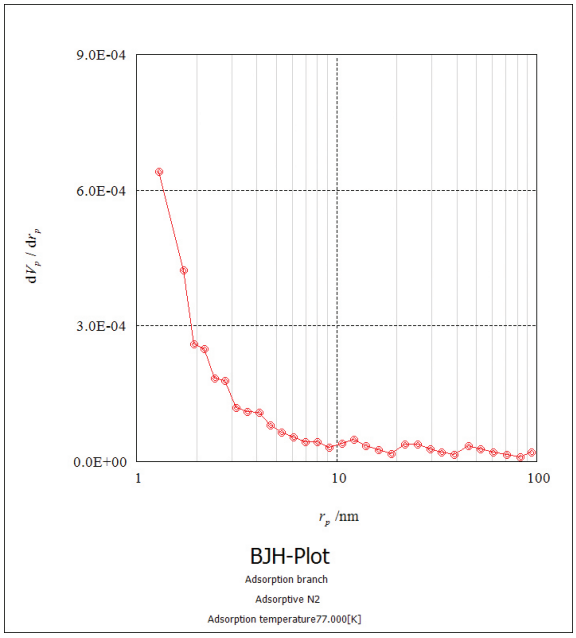

Fig. S4. BJH plot of NICSW.